# Structure and Function of the Long Pentraxin PTX3 Glycosidic Moiety: Fine-Tuning of the Interaction with C1q and Complement Activation

Antonio Inforzato,[‡] Giuseppe Peri,[§] Andrea Doni,[§] Cecilia Garlanda,[§] Alberto Mantovani,[§] Antonio Bastone,[||] Andrea Carpentieri,[⊥] Angela Amoresano,[⊥] Piero Pucci,[⊥] Anja Roos,[#] Mohamed R. Daha,[#] Silvia Vincenti,[▽] Grazia Gallo,[▽] Paolo Carminati,[▽] Rita De Santis,[▽] and Giovanni Salvatori*[,▽]

*Department of Biology, University "Tor Vergata", Rome, Italy, Istituto Clinico Humanitas (ICH), Rozzano, Milan, Italy, Istituto Ricerche Farmacologiche "Mario Negri", Milan, Italy, Department of Organic Chemistry and Biochemistry, University "Federico II", Naples, Italy, Department of Nephrology, Leiden University Medical Center, Leiden, The Netherlands, and Sigma-Tau R&D, Pomezia, Rome, Italy*

*Received April 18, 2006; Revised Manuscript Received June 27, 2006*

ABSTRACT: The prototypic long pentraxin PTX3 is a unique fluid-phase pattern recognition receptor that plays a nonredundant role in innate immunity and female fertility. The PTX3 *C*-terminal domain is required for C1q recognition and complement activation and contains a single N-glycosylation site on Asn 220. In the present study, we characterized the structure of the human PTX3 glycosidic moiety and investigated its relevance in C1q interaction and activation of the complement classical pathway. By specific endo and exoglycosidases digestion and direct mass spectrometric analysis, we found that both recombinant and naturally occurring PTX3 were N-linked to fucosylated and sialylated complex-type sugars. Interestingly, glycans showed heterogeneity mainly in the relative amount of bi, tri, and tetrantennary structures depending on the cell type and inflammatory stimulus. Enzymatic removal of sialic acid or the entire glycosidic moiety equally enhanced PTX3 binding to C1q compared to that in the native protein, thus indicating that glycosylation substantially contributes to modulate PTX3/C1q interaction and that sialic acid is the main determinant of this contribution. BIAcore kinetic measurements returned decreasing $K_{off}$ values as sugars were removed, pointing to a stabilization of the PTX3/C1q complex. No major rearrangement of PTX3 quaternary structure was observed after desialylation or deglycosylation as established by size exclusion chromatography. Consistent with C1q binding, PTX3 desialylation enhanced the activation of the classical complement pathway, as assessed by C4 and C3 deposition. In conclusion, our results provided evidence of an involvement of the PTX3 sugar moiety in C1q recognition and complement activation.

The long pentraxin PTX3 is an acute-phase glycoprotein of 45 kDa with glycosylation accounting for about 10% of its molecular weight (*1*). The protein is secreted by natural immunity cells and by several somatic cell types in response to either the inflammatory cytokines interleukin-1 $\beta$ (IL-1$\beta$)[1] and tumor necrosis factor α (TNFα) or the selected pathogen-associated molecular patterns (PAMPs) (*2*−*4*).

Like other members of the pentraxin family, PTX3 has a complex oligomeric structure with protomers linked to each other by disulfide bonds (*5*). PTX3 shares functional similarities with both short pentraxins CRP (C-reactive protein) and SAP (serum amyloid P component). It is involved in host defense against pathogen infection, in the regulation of the scavenger activity of macrophages and dendritic cells (DC), and in modulation of complement activity by binding to C1q (*6*−*8*). More recently, other functions have been characterized regarding the involvement of PTX3 in matrix deposition by cumulus cells (*9*) and the inhibition of angiogenesis by PTX3 interaction to fibroblast growth factor-2 (FGF-2) (*10*).

To date, little is known about the type of oligosaccharides linked to PTX3, and no data are available on the functional role of PTX3 glycosylation. Oligosaccharides may affect protein activity in various ways: they can mask a large region of the molecule to ligand recognition, participate in protein folding, and define binding sites on the protein surface (*11*−*15*). Inflammation can induce significant changes in the oligosaccharides of acute phase proteins (*16*, *17*), and the

[†] This work was financially supported by the Ministero Istruzione, Università e Ricerca (MIUR) application number 6669.

* To whom correspondence should be adressed. Tel: 06 9139 3847. Fax: 06 9139 3988. E-mail: giovanni.salvatori@sigma-tau.it.

[‡] University "Tor Vergata".

[§] Istituto Clinico Humanitas (ICH).

[||] Istituto Ricerche Farmacologiche "Mario Negri".

[⊥] University "Federico II", Naples.

[#] Leiden University Medical Center.

[▽] Sigma-Tau R&D.

[1] Abbreviations: IL-1$\beta$, interleukin-1 $\beta$; TNFα, tumor necrosis factor α; PAMPs, pathogen-associated molecular patterns; CRP, C reactive protein; SAP, serum amyloid P component; DC, dendritic cells; FGF-2, fibroblast growth factor-2; ER, endoplasmic reticulum; CHO, chinese hamster ovary; LPS, lipopolysaccharide; PTX3r, recombinant human PTX3; $PTX3_{8387}$, PTX3 from human fibrosarcoma cells 8387; $PTX3_{DC}$, PTX3 from human peripheral blood monocyte-derived DC.; endo F3-PTX3, endoglycosidase F3-treated PTX3; asialo-PTX3, α-(2→3, 6, 8, 9)-neuraminidase-treated PTX3; PSD, post source decay; EI, electron ionization; NeuNAc, *N*-acetylneuraminic acid; Gal, galactose; GlcNAc, *N*-acetylglucosamine; Fuc, fucose; GalNAc, *N*-acetylgalactose; Man, mannose; TIC, total ion current; SEC, size exclusion chromatography; CCP, classical complement pathway.

10.1021/bi0607453 CCC: $33.50 
Published on Web 08/30/2006

variation in protein glycosylation is a diagnostic indicator of a number of diseases (*18*, *19*).

Pentraxins are a family of proteins described to be variably glycosylated among species (*20*). It has recently been found that human SAP, known to be homogeneously glycosylated (*21*), can show microheterogeneity at the level of its complex biantennary oligosaccharides because of the loss of one or both terminal sialic acid residues (*22*). It is noteworthy that following desialylation SAP oligosaccharide chains exhibit a new orientation that determines conformational changes in protein tertiary and quaternary structures (*23*, *24*). Human CRP has been traditionally described as an unglycosylated protein (*25*). Surprisingly, it has been recently reported that different pathological conditions induce a novel glycosylation of the protein (*26*) and that differentially glycosylated CRPs exhibit variable binding to known ligands (*27*). These data indicate that the glycosylation status of pentraxins might contribute to the definition of their structural and biological properties and emphasizes the importance of further explorations of the role exerted by oligosaccharides in other members of the family.

We investigated the structure and functional role of the human PTX3 glycosidic moiety using proteins from three different sources: the recombinant PTX3 produced in a chinese hamster ovary (CHO) cell line, the protein from human peripheral blood monocyte-derived DC stimulated with lipopolysaccharide (LPS), and that from human fibrosarcoma cells 8387 stimulated with TNFα. We found that PTX3 was mainly N-linked to fucosylated and sialylated biantennary complex-type sugars. PTX3 glycans showed heterogeneity in the relative amount of bi, tri, and tetrantennary structures depending on cell type and inflammatory stimulus. Enzymatic deglycosylation or desialylation equally enhanced (2−3-fold) PTX3 binding to C1q compared to that in the unmodified protein. Consistent to C1q binding, the selective removal of sialic acid increased the PTX3-dependent activation of the classical complement pathway 2-fold, as assessed by C3 and C4 deposition. Thus, we provide evidence that PTX3 glycosylation status is directly implicated in the protein biological function and tunes the action of this prototypic long pentraxin.

## MATERIALS AND METHODS

*Purified Proteins*. Recombinant human PTX3 ($PTX3_r$) was purified from CHO cells stably and constitutively expressing the protein as described (*1*). Naturally occurring protein was purified by immunoaffinity from human fibrosarcoma cells 8387 exposed to TNF-α (20 ng/mL) for 24 h ($PTX3_{8387}$) and from human peripheral blood monocyte-derived DC stimulated with 100 ng/mL of LPS for 24 h ($PTX3_{DC}$) as previously described (*28*, *4*). In both cases, PTX3 was purified using the monoclonal antibody MNB4 cross-linked to a Protein G Sepharose column according to the manufacturer's instructions. C1q from human serum was available from Calbiochem, La Jolla, CA.

*Enzymes and Chemicals*. PNGase F and endoglycosidases F1, F2, and F3 (from *Chryseobacterium meningoseptum*), α-(2→3,6,8,9)-neuraminidase (from *Arthrobacter ureafaciens*), β-(1→4)-galactosidase and β-*N*-acetylglucosaminidase (from *Streptococcus pneumoniae*), proteomics grade trypsin (from porcine pancreas), bovine serum albumin (BSA), phosphate buffered saline (PBS) tablets, Triton X-100, Tween 20, 3,3′,5,5′-tetramethylbenzidine (TMB), dithiothreitol (DTT), and iodoacetamide were purchased from Sigma Aldrich, St. Louis, MO. LPS (*Escherichia coli* 055:B5) was from Difco, Detroit, MI, and TNFα was from BASF/Knoll, Ludwigshafen, Germany. Electrophoresis reagents were obtained from Bio-Rad, Hercules, CA. The 96-well microtiter plates were from Nunc, Roskilde, Denmark. The Protein G Sepharose 4 fast flow was purchased from Amersham Pharmacia Biotech, Uppsala, Sweden. Prepacked $C_{18}$ Sep-Pak cartridges were from Waters, Milford, MA. All other reagents and solvents were from Carlo Erba, Rodano, Italy and of the highest purity available.

*Antibodies.* Biotin-labeled rabbit anti-human PTX3 polyclonal antibody αPTX3pb and rat anti-human PTX3 monoclonal antibody MNB4 were obtained from "Mario Negri" Pharmacological Research Institute, Milan, Italy. Horseradish peroxidase (HRP)-conjugated streptavidin was purchased from Amersham Pharmacia Biotech. Goat anti-human C1q polyclonal antibody was from Calbiochem. Rabbit anti-goat IgG conjugated to HRP was from Sigma Aldrich. Mouse anti-human C1q monoclonal antibody mAb85 and Dig-conjugated mouse anti-human C4 monoclonal antibody C4-4a and anti-human C3 monoclonal antibody RFK22 were obtained from Leiden University Medical Center, Leiden, The Netherlands. HRP-conjugated F(ab′)2 from goat anti-Dig polyclonal antibody was purchased from Roche, Mannheim, Germany.

*Gel Electrophoresis*. Polyacrylamide gels (8.5%), along with sodium dodecyl sulfate (SDS), were put through a Laemmli (*29*) discontinuous buffer system. The gels were stained with Coomassie Brilliant Blue or silver nitrate (*30*).

*PNGase F Digestion*. PNGaseF digestion was carried out on $PTX3_r$, $PTX3_{8387}$, and $PTX3_{DC}$. Protein samples (5 μg) in PBS (10 mM phosphate buffer, 2.7 mM potassium chloride, 137 mM sodium chloride at pH 7.4) were first made 0.1% in SDS and 0.05 M in β-mercaptoethanol, then heated at 95 °C for 5 min. After the addition of Triton X-100 to a final concentration of 1%, the protein was incubated with 5 mU of PNGase F in a volume of 15 μL. Following 3 h of incubation at 37 °C, the samples were analyzed by SDS−PAGE.

*Endo and Exoglycosidase Analysis*. Endoglycosidase reactions were performed with *Chryseobacterium* endoglycosidases F1, F2, and F3. $PTX3_r$, $PTX3_{8387}$, and $PTX3_{DC}$ were first dialyzed against 50 mM sodium phosphate at pH 5.5 and then incubated in separate reactions with 1 mU of endoglycosidase F1, F2, or F3 per μg of protein. Hydrolysis proceeded for 16 h at 37 °C, and then the products were analyzed by SDS−PAGE. $PTX3_r$ samples treated with endoglycosidase F3 (endo F3-$PTX3_r$) were purified by size exclusion chromatography. Eluted proteins were quantitated by Lowry (*31*) and assayed for C1q binding activity. Exoglycosidase digestions were carried out as outlined for PNGase F deglycosylation, except for enzyme/substrate ratios. α-(2→3,6,8,9)-Neuraminidase (1 mU), β-(1→4)-galactosidase (1 mU), and β-*N*-acetylglucosaminidase (10 mU) per μg of protein were used singularly or differently combined. In another set of experiments, $PTX3_r$, $PTX3_{8387}$, and $PTX3_{DC}$ samples were desialylated under nondenaturing conditions (asialo-PTX3). Reactions were performed in PBS for 16 h at 37 °C, using 2 mU of α-(2→3,6,8,9)-neuramini-

dase per $\mu$g of protein. Following SDS−PAGE analysis, the reaction products were purified and assayed for C1q binding activity as described above for endo F3-PTX3$_r$.

*Isolation of N-Linked Oligosaccharides*. PTX3$_r$ (300 $\mu$g) was reduced and alkylated as previously described (*32*). Aliquots of the reduced and carboxymethylated protein were digested overnight with trypsin in 50 mM ammonium bicarbonate (pH 8.5) at 37 °C using a 1:50 enzyme/substrate ratio (w/w). Samples were then diluted with water and lyophilized. Deglycosylation of the peptide mixture was performed overnight by treatment with 100 mU of PNGase F per 300 $\mu$g of protein in 50 mM ammonium bicarbonate (pH 8.5) at 37 °C. The N-linked oligosaccharides were separated from the peptides by reverse-phase chromatography on prepacked $C_{18}$ Sep-Pak cartridges (*33*).

*Methanolysis and Chemical Derivatization for GC-MS Analysis*. PTX3$_r$ (200 $\mu$g) was dissolved in 500 $\mu$L of 1 M methanolic-HCl at 80 °C for 16 h. The re-N-acetylation of the monosaccharide mixture was performed by adding 500 $\mu$L of methanol, 10 $\mu$L of pyridine, and 50 $\mu$L of acetic anhydride at room temperature for 15 min. Sugars were finally trimethylsilylated in 200 $\mu$L of *N*,*O*-bis-(trimethylsilyl)-acetamide (TMSA) at 70 °C for 15 min. The sample was dried under nitrogen, dissolved in 50 $\mu$L of hexane, and centrifuged to remove any excess solid reagent. The hexane supernatant (1/60) was used for GC-MS analysis.

*MALDI-MS Analysis*. Both positive and negative MALDI-MS analyses and MALDI-PSD experiments were carried out on a Voyager DE STR Pro instrument operating in reflectron mode (Applied Biosystems, Framingham, MA). The MALDI matrixes were prepared by dissolving 10 mg of 2,5-dihydroxybenzoic acid (2,5-DHB) in 1 mL of methanol or 10 mg of α-cyano-4-hydroxycinnamic acid (HCCA) in 1 mL of acetonitrile/0.2% trifluoroacetic acid (TFA) (70:30 v/v). Typically, 1 $\mu$L of the matrix was applied to the metallic sample plate, and 1 $\mu$L of analyte was then added. Acceleration and reflector voltages were set up as follows: target voltage at 20 kV, first grid at 66% of target voltage, and delayed extraction at 200 ns. The PSD fragment spectra were acquired after pseudomolecular cation selection using a time ion selector. Fragment ions were refocused by a 20% stepwise reduction of reflector voltage. The individual segments were then stitched together using Applied Biosystems software. Raw data were analyzed using computer software provided by the manufacturers and are reported as monoisotopic masses.

*GC-MS Analysis*. GC-MS analyses were performed on a Hewlett-Packard 5890 instrument under the following conditions: ZB-5 capillary column (Phenomenex, 30 m × 0.25 mm i.d., flow rate 0.8 mL/min, He as carrier gas). The injection temperature was 250 °C. For sugar analyses, the oven temperature was increased from 25 to 90 °C in 1 min and kept at 90 °C for 1 min before increasing to 140 °C at 25 °C/min, to 200 °C at 5 °C/min, and finally to 300 °C at 10 °C/min. Electron ionization (EI) mass spectra were recorded by continuous quadrupole scanning at 70 eV ionization energy.

*C1q Binding Assays*. PTX3$_r$, PTX3$_{8387}$, PTX3$_{DC}$, and the corresponding desialylated and deglycosylated proteins were assayed for their C1q binding activity in direct binding assays. The 96-well plates were coated overnight at 4 °C with 50 ng/well of C1q in PBS. All reaction volumes were 100 $\mu$L, and the plates were washed after each step with PBS containing 0.1% v/v Triton X-100. The wells were blocked with PBS containing 0.1% v/v Triton X-100 and 1% w/v BSA for 2 h at room temperature. Protein samples were diluted in blocking solution and added to the wells. Binding was then carried out for 1 h at room temperature. After extensive washing, the plates were incubated with the αPTX3pb polyclonal antibody (1:10000 in PBS, 0.1% Triton X-100, 1% BSA; 1 h at room temperature) followed by HRP-labeled streptavidin (1:4000 in PBS, 0.1% Triton X-100, 1% BSA; 1 h at room temperature). Finally, TMB was added as a chromogen substrate for HRP, and absorbance values were read at 450 nm. The binding of PTX3$_r$ to C1q was also assessed by inhibition experiments. The plates were coated overnight at 4 °C with PTX3$_r$ or asialo-PTX3$_r$ (100 $\mu$L/well of a 1 $\mu$g/mL solution in 50 mM sodium carbonate at pH 9.6). All reaction volumes were 100 $\mu$L, and the plates were washed after each step with PBS containing 0.05% v/v Tween 20. The wells were blocked with PBS containing 0.05% v/v Tween 20 and 1% w/v BSA for 1 h at 37 °C; in a separate 96-well cell culture plate, the mixtures of a fixed amount of C1q (5 $\mu$g/mL in blocking solution) and serial dilutions of PTX3$_r$ or asialo-PTX3$_r$ (from 5 $\mu$g/mL to 80 ng/mL in blocking solution) were preincubated for 1 h at 37 °C. Then mixtures were added to either PTX3$_r$- or asialo-PTX3$_r$-coated wells, incubation was prolonged for another hour at 37 °C. Following extensive washing, bound C1q was revealed using the anti-C1q polyclonal antibody (1:5000 in blocking solution) followed by HRP-labeled secondary antibody (1:4000 in blocking solution). Binding was detected as indicated above. Raw data were analyzed by the SigmaPlot statistics package (version 7.101, Systat Software, Point Richmond, CA), and the results were expressed as both inhibition percentages (relative to free C1q) and IC50 values (protein concentration that inhibits 50% C1q binding). endo F3-PTX3$_r$ was assayed in a similar experimental setting.

*Complement Activation*. Activation of complement via PTX3$_r$ and asialo-PTX3$_r$ was assessed as described (*8*). Briefly, microtiter wells were coated with PTX3$_r$, asialo-PTX3$_r$, purified human IgM, or BSA and blocked by BSA. Subsequently, the plates were incubated with NHS as a complement source, diluted in GVB$^{+/+}$ (1.8 mM sodium 5,5-diethylbarbital, 0.2 mM 5,5-diethylbarbituric, 145 mM NaCl, 2 mM $CaCl_2$, 5 mM $MgCl_2$, 0.05% Tween 20, and 0.1% gelatin) and incubated for 1 h at 37 °C. In some experiments, NHS was diluted in GVB$^{+/+}$ containing 5 $\mu$g/mL of mAb85 in a calcium-free buffer (GVB$^{+/-}$/MgEGTA: 1.8 mM sodium 5,5-diethylbarbital, 0.2 mM 5,5-diethylbarbituric, 145 mM NaCl, 5 mM $MgCl_2$, 10 mM EGTA, 0.05% Tween 20, and 0.1% gelatin) or in a calcium- and magnesium-free buffer (GVB$^{-/-}$/EDTA: 1.8 mM sodium 5,5-diethylbarbital, 0.2 mM 5,5-diethylbarbituric, 145 mM NaCl, 10 mM EDTA, 0.05% Tween 20, and 0.1% gelatine). The deposition of C3 and C4 was detected by Dig-conjugated RFK22 and C4-4a, respectively. To determine the effect of desialylation on PTX3 complement activation, a C1q-dependent haemolytic assay was performed in the presence of increasing concentrations of PTX3$_r$ and asialo-PTX3$_r$ as described earlier (*34*).

*Size Exclusion Chromatography*. PTX3, asialo-PTX3, or endo F3-PTX3 was purified by size exclusion chromatography. Protein samples in PBS were applied to a Superose 6 column (Amersham Pharmacia Biotech) calibrated with

molecular weight standards and eluted with PBS at a flow rate of 0.4 mL/min. Elution was monitored by UV detection at 280 nm.

*ELISA*. PTX3, asialo-PTX3, and endo F3-PTX3 were dosed with a sandwich ELISA on the basis of the monoclonal antibody MNB4 and the rabbit polyclonal antibody αPTX3pb (*4*).

*Biosensor Analysis*. The interaction with C1q of $PTX3_r$, asialo-$PTX3_r$, or endo F3-$PTX3_r$ was also analyzed through a BIAcore system (biomolecular interaction analysis; BIAcore AB, Uppsala, Sweden). C1q was immobilized on a CM5 sensor chip (BIAcore AB) using the amine coupling kit (BIAcore AB). A volume of 35 $\mu$L of the ligand (50 $\mu$g/mL of C1q in 10 mM MES at pH 6.1) was immobilized with a continuous flow of HBS (10 mM HEPES, 150 mM NaCl, 3.4 mM EDTA, 0.05% BIAcore surfactant P20 at pH 7.4) at 5 $\mu$L/min. Each binding assay was performed with a constant flow rate (25 $\mu$L/min) of HBS (pH 7.4) at 25 °C. The analytes were injected over the ligand surface in HBS, and the surface was then regenerated by injection of 25 $\mu$L of 5 mM NaOH. Kinetic analyses were performed with serial dilutions of the analytes in HBS to concentrations ranging from 20 to 200 nM. Each sample was injected and allowed a total contact time of 4 min with the ligand surface.

*Homology Modeling*. The primary sequence of the human PTX3 *C*-terminus domain shares 28% identity with the overall sequence of human CRP. A 3D model of the human PTX3 *C*-terminus domain (aa 178−381) was thus built using the crystallographic structure of human CRP as a template (*35*) (pdb code: 1B09). Multialignment was performed using ClustalW (http://www2.ebi.ac.uk/clustalw/) and then refined by hand to localize insertions and deletions out of conserved secondary structures. SwissPDB software (http://www.expasy.org/spdbv/) was utilized to obtain a preliminary 3D model. The conserved disulfide bond, between Cys210 and Cys271, was imposed as the constraint. Structure optimization was performed by molecular dynamics (force field OPLS-AA in water, 200 ps at 300 K, using a 300 kJ $mol^{-1}$ $Å^{-2}$ constraint on $\beta$-strand and α-helical motives), and 20 structures were extracted and minimized using SD and TNCG algorithms up to a convergence criterion of $5 \times 10^{-3}$ kJ $mol^{-1}$ $Å^{-1}$. The best solution in terms of the percentage of amino acids in the most favorite and allowed regions was chosen using the utility Procheck (http://www.biochem.ucl.ac.uk/~roman/**procheck**/**procheck**.html).

*Conformational Analysis of Biantennary Oligosaccharides*. A core-monofucosylated and disialylated biantennary oligosaccharide was built using the scheme reported in Figure 8A and linked to Asn220. Psi and Phi values for each disaccharide unit were extracted from the Glytorsion database (http://www.glycosciences.de/tools/glytorsion/). We performed a dihedral angle driving conformational analysis, rotating every 30° the torsion angles chi1 and chi2 on Asn220 and phi on the first GlcNAc of the oligosaccharide chain. The four most diverse conformations, in contact with the protein, were then submitted to a Metropolis Monte Carlo/Stochastic Dynamics procedure (MC/SD) (force field OPLS-AA in water, 100 dynamics time step = 100 fs every Monte Carlo trial, up to 1 ns). A combination of 2−4 torsion angles, phi and psi of each disaccharide, were allowed to randomly rotate every 30°. This protocol could guarantee an acceptance ratio >10%. All side chains of the amino acids within a distance of 28 Å from the first mannose were kept free. The same calculations were performed using as input a core-monofucosylated desialylated biantennary oligosaccharide. One hundred conformations for each initial input were retained, minimized, and then clustered to choose the most representative ones. All calculations were performed using the software Macromodel (version 8.6, Schrodinger L. L. C., Portland, OR).

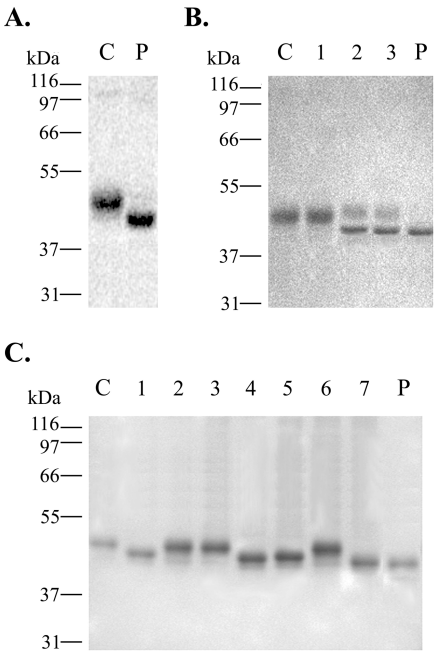


FIGURE 1: SDS−PAGE analysis of endo and exoglycosidase-treated $PTX3_r$. (A) Purified $PTX3_r$ was incubated with PNGase F under denaturing conditions and then analyzed on a 8.5% SDS polyacrylamide gel (lane P). The untreated protein is shown in lane C. (B) $PTX3_r$ samples were subjected to hydrolysis with endoglycosidase F1 (lane 1), endoglycosidase F2 (lane 2), or endoglycosidase F3 (lane 3) under nondenaturing conditions in 50 mM sodium phosphate at pH 5.5. The electrophoretic mobility produced by the reaction products were compared to that of the untreated protein (lane C) and the PNGase F deglycosylated $PTX3_r$ (lane P), as in A. (C) Following SDS denaturation and $\beta$-mercaptoethanol reduction, $PTX3_r$ was incubated with α-(2→3,6,8,9)-neuraminidase (lane 1), $\beta$-(1→4)-galactosidase (lane 2), or $\beta$-*N*-acetylglucosaminidase (lane 3). Enzymes were also combined two by two (lane 4, α-(2→3,6,8,9)-neuraminidase and $\beta$-(1→4)-galactosidase; lane 5, α-(2→3,6,8,9)-neuraminidase and $\beta$-*N*-acetylglucosaminidase; lane 6, $\beta$-(1→4)-galactosidase and $\beta$-*N*-acetylglucosaminidase), or all three were used (lane 7). The extent of deglycosylation was monitored in comparison to that of the untreated (lane C) and PNGase F deglycosylated proteins (lane P), as in B.

## RESULTS

*Endo and Exoglycosidase Analyses.* It was reported in a previous investigation that PTX3 primary sequence shows a single potential N-glycosylation site at amino acid position 220 (*1*). To better characterize the PTX3 glycosylation status, the protein was treated with substrate-specific endo and exoglycosidases (Table 1), and the extent of deglycosylation was monitored as an increase in electrophoretic mobility in SDS−PAGE.

PNGaseF, an enzyme that cleaves Asn-linked high mannose as well as hybrid and complex oligosaccharides (*36*), reduced the apparent molecular weight of $PTX3_r$ (Figure 1A) from 45 to 40 kDa, thus confirming the presence of N-linked glycans.

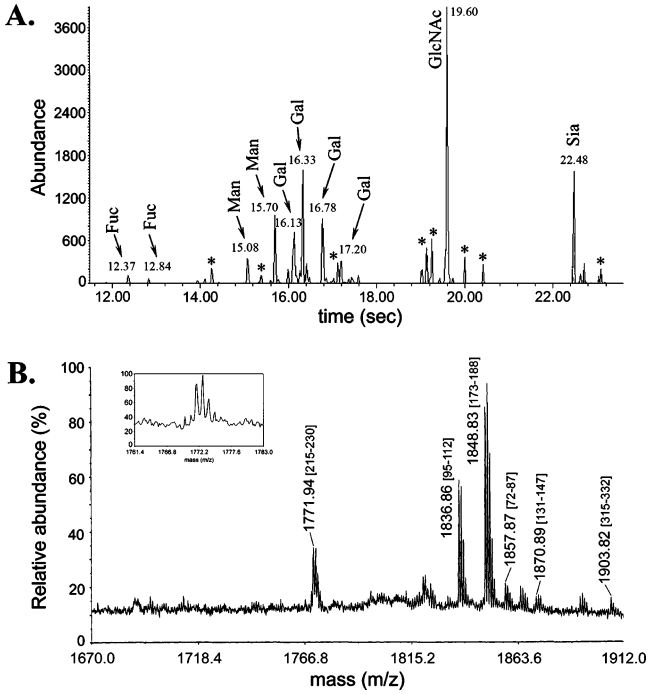


FIGURE 2: Monosaccharide composition and site occupancy analysis of $PTX3_r$ sugars. (A) $PTX3_r$ oligosaccharides were reduced to constituent monosaccharides by methanolysis. Trimethylsilyl-derivatives were separated on a GC column and identified by characteristic fragmentation patterns in electron ionisation (EI) mass spectrometry. The corresponding total ion current (TIC) chromatogram showed the appearance of peaks representative of the specified residues. Contaminants are referred to with asterisks. (B) $PTX3_r$ was reduced and alkylated, then subjected to trypsin digestion; the resulting peptide mixture was deglycosylated by PNGase F treatment and directly analyzed by MALDI-MS operating in positive ion mode. The mass signals recorded in the spectrum were assigned to the corresponding peptides within the PTX3 sequence (in brackets) on the basis of their mass value and trypsin specificity. Only the portion of the spectrum spanning the molecular mass of the peptide 215−230, containing the unique N-glycosylation site, is shown. An expanded view showing the isotopic pattern of the mass signal at *m*/*z* 1771.94 is shown in the insert.

To establish the general type of $PTX3_r$ sugars, we evaluated their reactivity toward the *Chryseobacterium* endoglycosidases F1, F2, and F3. These enzymes cleave the glycosidic bond between the two GlcNAc residues in the diacetylchitobiose core with type-dependent specificity (Table 1). Because endoglycosidases F1, F2, and F3 are less sensitive to protein conformation than PNGase F (*36*), the reactions were performed in nondenaturing conditions. The resistance of $PTX3_r$ to endoglycosidase F1 deglycosylation (Figure 1B, lane 1) indicates that neither high mannose nor hybrid oligosaccharides are linked to the protein. As a positive control of enzyme activity, carboxypeptidase Y, a glycoprotein carrying only high mannose N-linked glycans (*37*), was effectively deglycosylated by endoglycosidase F1 (data not shown). Treatment of $PTX3_r$ with both endoglycosidases F2 and F3 (Figure 1B, lanes 2 and 3, respectively) produced a reduction of the apparent molecular weight comparable to that obtained after PNGase F deglycosylation, thus revealing the presence of complex-type oligosaccharides. Neither the F2 nor the F3 endoglycosidase completely removed glycosylation from $PTX3_r$ because a small amount of protein remained uncleaved at the molecular weight of 45 kDa. The specificity of endoglycosidase F2 for complex

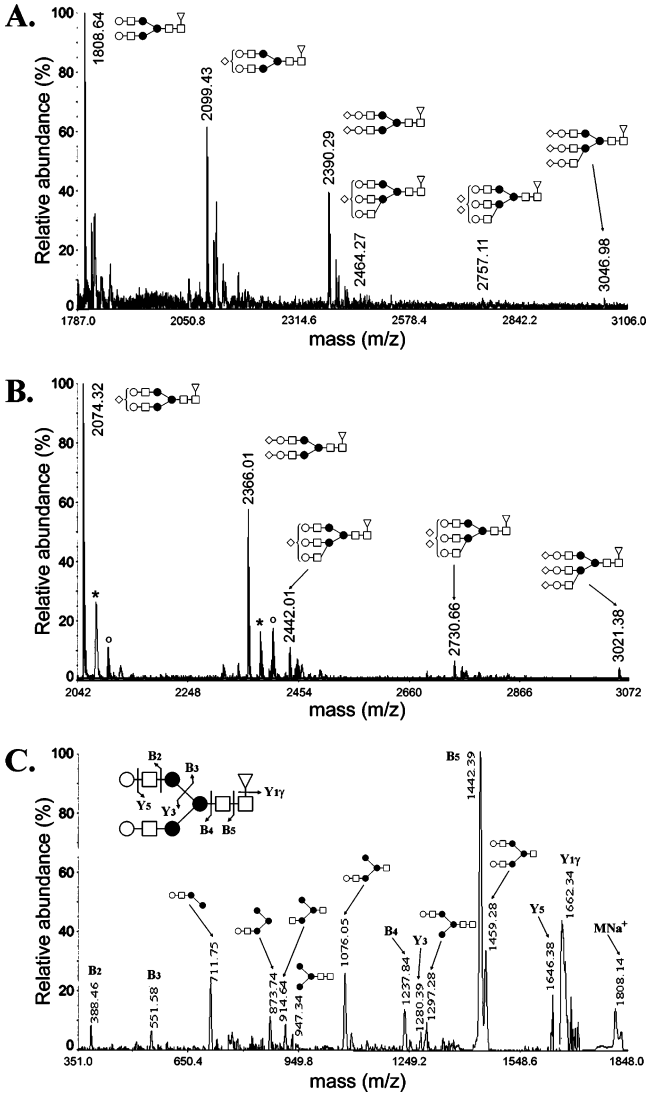


FIGURE 3: $PTX3_r$ sugar profiling and PSD fragmentation by MALDI-MS. Oligosaccharides were released from $PTX3_r$ polypeptide backbone by PNGase F digestion and directly analyzed by MALDI-MS both in positive (A) and negative (B) ion mode. Corresponding sodiated pseudomolecular ions were recorded in the positive MALDI-MS spectrum, whereas pseudomolecular anions were observed in the negative spectrum. Glycoform structures inferred by MS data are shown; satellite peaks in B are attributed to $Na^+$ (*) or $K^+$ (°) adducts. (C) The $MNa^+$ ion at *m*/*z* 1808.64 was selected as a precursor ion and submitted to PSD fragmentation. Y and B ions as well as fragments originated by double cleavages are indicated. Symbols are △, fucose; □, *N*-acetylglucosamine; ●, mannose; ○, galactose; ◇, *N*-acetylneuraminic acid.

biantennary structures indicates that the nondeglycosylated fraction of $PTX3_r$ is presumably conjugated to triantennary and tetrantennary oligosaccharides. No tetrantennary structures can be recognized from any of the endoglycosidases used, which can explain the persistence of a minor amount of glycosylated $PTX3_r$, even after the endoglycosidase F3 treatment. Taken together, these results indicate that the protein is conjugated to complex-type sugars with a prevalence of biantennary and a lower amount of tri and tetrantennary structures.

To confirm the complex type of $PTX3_r$ sugars and to further characterize the structural features of their antennae, we analyzed, in SDS−PAGE, the electrophoretic mobility of $PTX3_r$ subjected to treatment with specific exoglycosi-

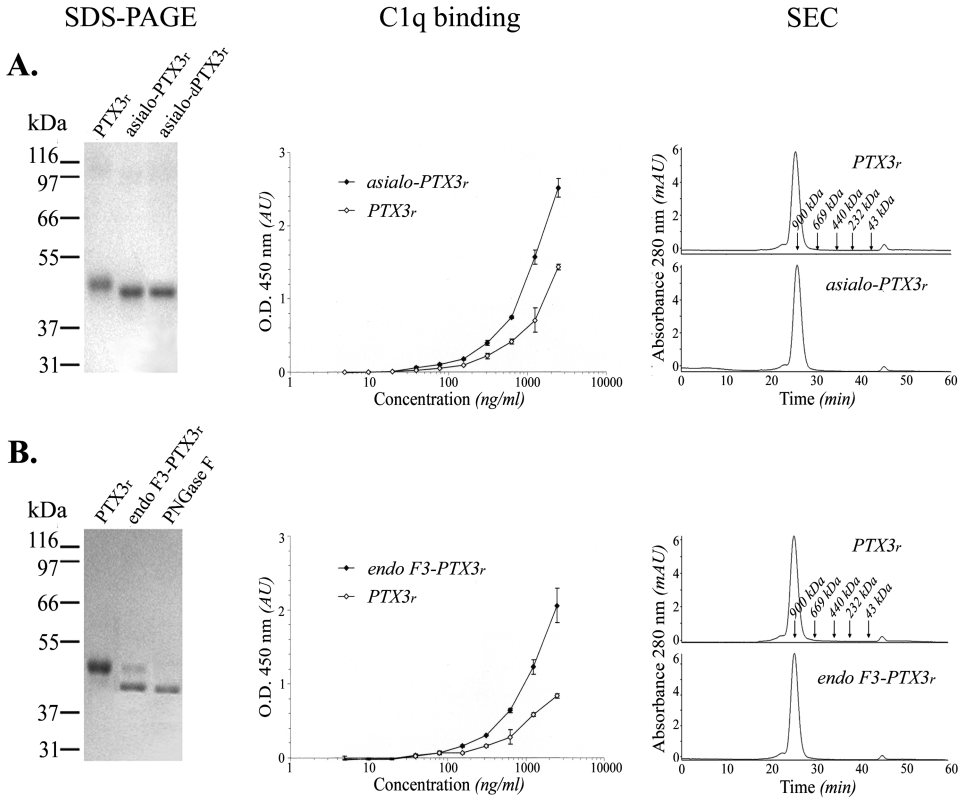


FIGURE 4: SDS−PAGE analysis, C1q binding, and SEC profile of asialo and endo F3-PTX3$_r$. (A) Left panel: PTX3$_r$ was incubated with α-(2→3,6,8,9)-neuraminidase under nondenaturing conditions. The extent of sialic acid removal was assessed in SDS−PAGE in comparison to the same reaction performed under denaturing conditions (asialo-dPTX3$_r$). Middle panel: asialo-PTX3r and PTX3r were serially diluted to a concentration ranging from 5000 to 10 ng/mL and then added to C1q-coated wells. Data shown are representative of at least three independent experiments. Right panel: elution profiles of asialo-PTX3$_r$ and PTX3$_r$ in size exclusion chromatography. Arrows indicate molecular weight standards (ovalbumin, 43 kDa; catalase, 232 kDa; ferritin, 440 kDa; thyroglobulin, 669 kDa; rabbit IgM, 900 kDa). (B) Left panel: PTX3$_r$ was subjected to incubation with endoglycosidase F3 under nondenaturing conditions. Endo F3-PTX3$_r$ was analyzed in SDS−PAGE and compared to the protein deglycosylated with PNGase F under denaturing conditions (PNGase F). C1q binding assay (middle panel) and SEC analysis (right panel) were performed as described above for asialo-PTX3$_r$.

dases (Table 1). The incubation of PTX3$_r$ with α-(2→3,6,8,9)-neuraminidase produced a slight but appreciable increase in protein electrophoretic mobility (Figure 1C, lanes 1), thus indicating terminal residues of sialic acid. The treatment of PTX3$_r$ with either *β*-(1→4)-galactosidase or *β*-*N*-acetylglucosaminidase let the protein's apparent molecular weight unmodified (Figure 1C, lanes 2 and 3, respectively). Incubation with α-(2→3,6,8,9)-neuraminidase and *β*-*N*-acetylglucosaminidase (Figure 1C, lane 5) produced an increase in the PTX3$_r$ electrophoretic mobility similar to that observed after treatment with α-(2→3,6,8,9)-neuraminidase, confirming the occurrence of terminal NeuNAc residues. Moreover, a mixture of *β*-(1→4)-galactosidase and *β*-*N*-acetylglucosaminidase was unable to modify the apparent molecular weight of PTX3$_r$ (Figure 1C, lanes 6), indicating that Gal and GlcNAc residues are protected from enzyme hydrolysis by NeuNAc monosaccharides at the nonreducing termini of the antennae. The incubation of PTX3$_r$ with a combination of α-(2→3,6,8,9)-neuraminidase and *β*-(1→4)-galactosidase or with all of the three exoglycosidases (Figure 1C, lanes 4 and 7, respectively) produced a greater reduction of the protein molecular weight than that observed after treatment of PTX3$_r$ with α-(2→3,6,8,9)-neuraminidase alone. These results are consistent with the general motif NeuNAc-Gal-GlcNAc, which is representative of complex-type sugar antennae and points out the presence of NeuNAc residues as capping sugars.

*Mass Spectrometry*. The carbohydrate moiety of PTX3$_r$ was submitted to detailed structural characterization by exploiting different mass spectrometric methodologies.

The monosaccharide composition of PTX3$_r$ glycans was determined by GC-MS analysis. The total ion current (TIC) profile (Figure 2A) showed the occurrence of Fuc, Man, Gal as well as GlcNAC, and NeuNAc residues. These data are consistent with the presence of complex-type glycans indicated by the endo and exoglycosidase analyses described above. Moreover, the appearance of Fuc signals suggests that PTX3$_r$ oligosaccharides are also fucosylated as well as sialylated. It is noteworthy that no GalNAc residues were observed by GC-MS analysis, which rules out the possibility of O-linked glycosylation.

The N-linked site occupancy was investigated by peptide mass fingerprinting following PNGaseF treatment. A PTX3$_r$ sample was reduced and alkylated, then digested with trypsin; the resulting peptide mixture was analyzed by MALDI-MS before and after PNGaseF hydrolysis. The mass signal at *m*/*z* 1771.94 was assigned to peptide 215−230 containing the unique N-glycosylation site and could only be detected following deglycosylation of the sample. The measured monoisotopic mass value increased by 1 Da compared to that expected (1770.96 Da) because Asn220 was converted into Asp by the enzymatic treatment, thus demonstrating the complete glycan occupancy at Asn220 (Figure 2B).

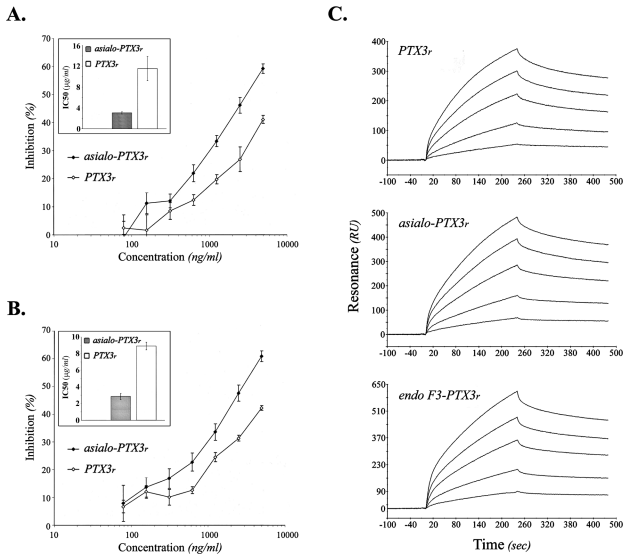


FIGURE 5: C1q inhibition assays and BIAcore analyses. (A) Preincubated mixtures of fixed amounts of C1q and serial dilutions of asialo-PTX3$_r$ or PTX3$_r$ were added to PTX3$_r$-coated wells. Bound C1q was revealed, and the results were expressed as both inhibition percentages (curves) and IC50 values (histogram in the insert). Data shown are representative of three independent experiments. (B) The wells were coated with asialo-PTX3$_r$, and inhibition experiments were performed as in A. (C) BIAcore saturation analysis of PTX3$_r$, asialo-PTX3$_r$ and endo F3-PTX3$_r$ binding to C1q. Increasing concentrations of PTX3 (from 20 to 200 nM) were allowed to interact with immobilized C1q (base value 18 890 RU) for 4 min, and association curves were recorded. Buffer was then run over and dissociation allowed to proceed. The kinetic parameters were calculated for each sensorgram; corresponding mean values (±standard error) are indicated in the text. Data are from a single experiment, representative of four performed.

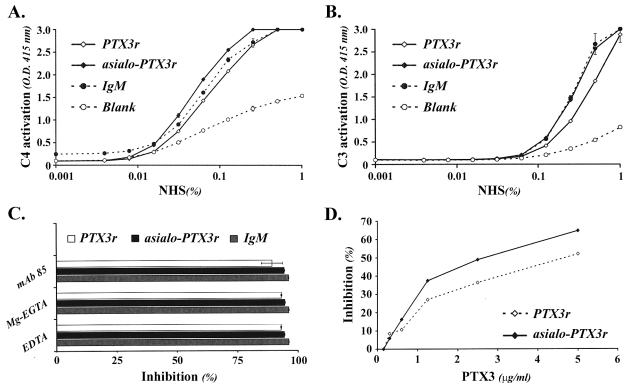


FIGURE 6: Complement activation on PTX3$_r$ and asialo-PTX3$_r$. (A and B) Wells were coated with PTX3$_r$, asialo-PTX3$_r$, IgM, or coating buffer (blank), followed by incubation with NHS and assessment of deposition of C4 (A) and C3 (B). (C) The plates were coated with PTX3$_r$, asialo-PTX3$_r$ or IgM and incubated with NHS in GVB$^{+/+}$, GVB$^{+/-}$/MgEGTA, GVB$^{-/-}$/EDTA, or with NHS in the presence of mAb85, and the deposition of C3 was assessed. (D) PTX3$_r$ or asialo-PTX3$_r$ was preincubated with purified C1q and tested in a C1q-dependent haemolytic assay. Data shown in A, B, and C are representative of three independent experiments; panel D shows the results from a single experiment, representative of three performed.

The oligosaccharide chains released from PTX3$_r$ by PNGaseF digestion were recovered and directly analyzed by MALDI-MS, both in positive and negative ion mode. Sugar profiling by positive MALDI-MS analysis revealed the occurrence of fucosylated and variably sialylated or not sialylated biantennary with minor triantennary structures, thus

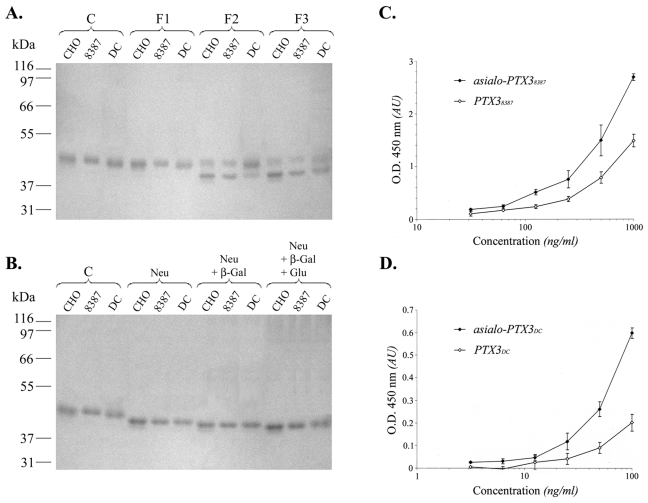


FIGURE 7: SDS−PAGE analysis and C1q binding of endo and exoglycosidase-treated PTX3 from natural sources. (A) PTX3 from fibrosarcoma 8387 (8387) and monocyte-derived dendritic cells (DC) was incubated with endoglycosidase F1 (F1), endoglycosidase F2 (F2), or endoglycosidase F3 (F3) under nondenaturing conditions. Digestions were carried out on the recombinant protein (CHO) as well. Reaction products were analyzed on a 8.5% SDS polyacrylamide gel, and the electrophoretic mobility was compared to that of the untreated proteins (C). (B) Proteins were incubated with α-(2→3,6,8,9)-neuraminidase (Neu), *β*-(1→4)-galactosidase (*β*-Gal), and *β*-*N*-acetylglucosaminidase (Glu) under denaturing conditions. The extent of deglycosylation was monitored in comparison to that of the untreated proteins (C), as in A. (C) Asialo-PTX3$_{8387}$ and PTX3$_{8387}$ were serially diluted to a concentration ranging from 1000 to 32 ng/mL and then added to C1q-coated wells. Bound proteins were revealed by αPTX3pb polyclonal antibody. Reported values are representative of three independent experiments. (D) Asialo-PTX3$_{DC}$ and PTX3$_{DC}$ were assayed as in C. Concentration values ranged from 100 to 3 ng/mL.

confirming that PTX3$_r$ oligosaccharides belong to the complex type (Figure 3A). However, because significant desialylation has been described to occur in positive ion mode (*38*), negative MALDI-MS analyses were also performed. Because the mass signals corresponding to nonsialylated biantennary structures disappeared in the acquired negative ion spectrum (Figure 3B), sialic acid residues were lost to a great extent in positive ion mode. The intensity ratios among the observed sialylated structures appeared to be essentially similar to those recorded in the positive MALDI spectra, confirming the sugar profiling described therein. To increase sensitivity of the mass spectral analysis, PTX3$_r$ oligosaccharides were finally examined following peracetylation, showing the presence of very minor tetrantennary structures with a different degree of sialylation (data not shown).

The ultimate definition of the different glycan structures including the sequence and branching degree of the antennae was achieved by tandem mass spectrometry analysis using MALDI-PSD techniques. The PSD spectra were dominated by Y and B ions containing the nonreducing or reducing ends of the glycans as well as a large number of internal fragment ions formed by multiple glycosidic cleavages. Sequence and branching information could be inferred by the interpretation of the fragmentation spectra. For example, Figure 3C shows the PSD spectrum obtained by selecting the precursor ion observed at *m*/*z* 1808.64 in the positive ion spectrum. The B5 ion at *m*/*z* 1442.39 resulting from the cleavage of the glycosidic bond between the two GlcNAc

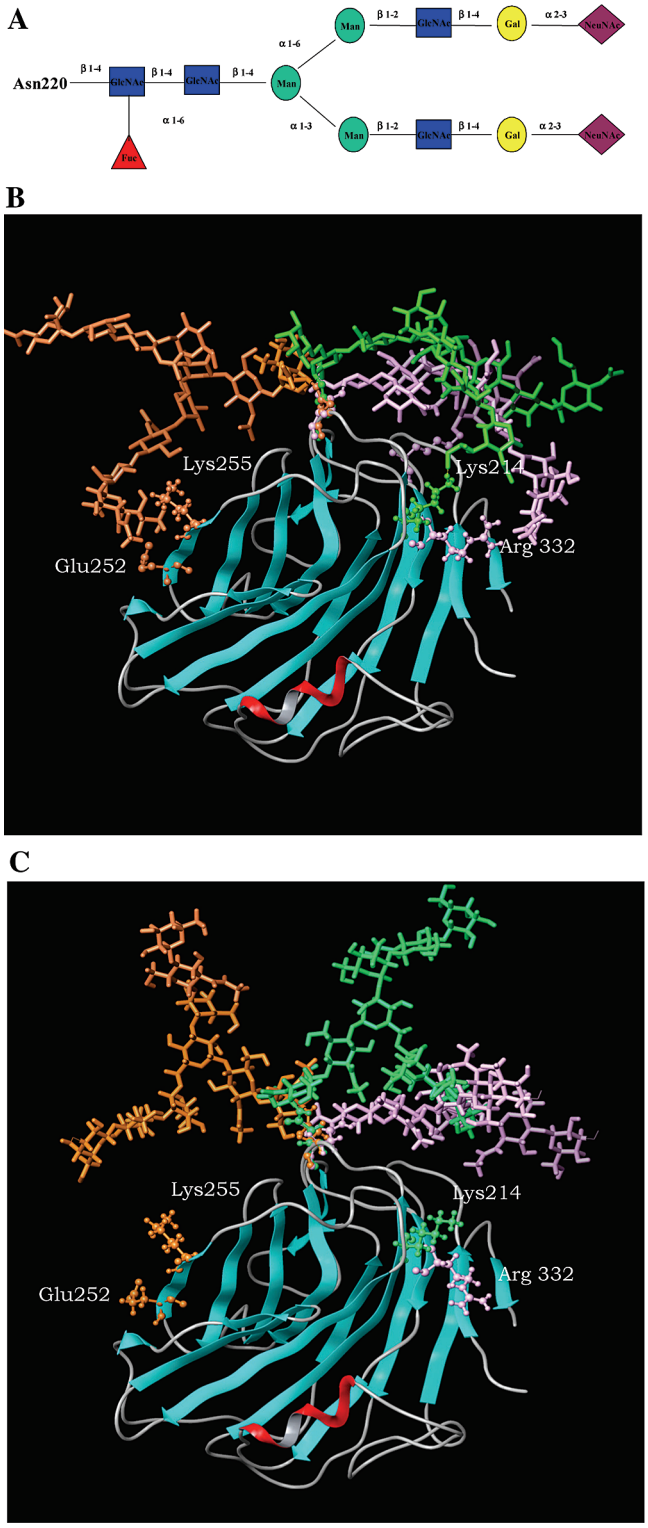


FIGURE 8: Representative conformations of a sialylated and desialylated biantennary oligosaccharide linked to the Asn220 of a 3D model of the PTX3 *C*-terminus domain. (A) Scheme of a core-monofucosylated and disialylated biantennary oligosaccharide. (B) Representative solutions of the sialylated oligosaccharide are reported in three different colors (orange, green, and purple). The structural model of the *C*-terminus domain of PTX3, built by a homology modeling procedure, is represented as a ribbon colored by secondary structure. Amino acid residues (ball-and-stick) contacting sialic acid are accordingly colored. (C) representative solutions of the desialylated oligosaccharide.

core residues led to the localization of the Fuc moiety on the first GlcNAc. On the whole, PSD data on the species at *m*/*z* 1808.64 identified a biantennary structure with a Fuc unit on the first GlcNAc core residue.

Table 1: Endo and Exoglycosidases Used in PTX3 Glycan Analysis.

| enzyme | EC | source | substrate |
|---|---|---|---|
| PNGase F | 3.5.1.52 | *Chryseobacterium meningoseptum* | All N-linked complex, hybrid, or high mannose oligosaccharides unless *β*-(1→3)-fucosylated[a] |
| endoglycosidase F1 | 3.2.1.96 | *Chryseobacterium meningoseptum* | N-linked high mannose and hybrid oligosaccharides[b] |
| endoglycosidase F2 | 3.2.1.96 | *Chryseobacterium meningoseptum* | N-linked high mannose and biantennary complex oligosaccharides[b] |
| endoglycosidase F3 | 3.2.1.96 | *Chryseobacterium meningoseptum* | N-linked biantennary and triantennary complex oligosaccharides[b] |
| α−(2→3,6,8,9)-neuraminidase | 3.2.1.18 | *Arthrobacter ureafaciens* | terminal nonreducing α-(2→3), α-(2→6), α-(2→8), and α-(2→9)-linked NeuNAc residues |
| *β*-(1→4)-galactosidase | 3.2.1.23 | *Streptococcus pneumoniae* | terminal nonreducing *β*-(1→4)-linked Gal residues |
| *β*-*N*-acetylglucos-aminidase | 3.2.1.52 | *Streptococcus pneumoniae* | terminal nonreducing *β*-(1→2) and *β*-(1→4)-linked GlcNAc residues. |

[a] PNGase F cleaves the N-glycosidic bond between the asparagine and the first GlcNAc residue in the diacetylchitobiose core. The enzyme works as an amidase with the asparagine being converted to aspartic acid. [b] Endoglycosidases F1, F2, and F3 cleave the O-glycosidic bond between the two GlcNAc residues in the diacetylchitobiose core, generating a truncated sugar molecule with one GlcNAc remaining on the peptide moiety.

*PTX3$_r$ Glycosylation Status Affects C1q Recognition*. The site of sugar attachment in PTX3 (Asn 220) is located on the pentraxin domain. Previous results indicate that this region of the protein is required for C1q recognition (*8*). To investigate the role of glycosylation on PTX3 biological activity, the interaction of PTX3 with C1q was studied. PTX3$_r$ was desialylated with α-(2→3,6,8,9)-neuraminidase under nondenaturing conditions. As shown in Figure 4A left panel, NeuNAc residues were extensively removed from PTX3$_r$ in both native and denaturing conditions. Deglycosylated PTX3$_r$ was produced by endoglycosidase F3 treatment (Figure 4B, left panel). Asialo-PTX3$_r$ and endo F3-PTX3$_r$ were then compared to the untreated protein for their C1q binding activity. In direct binding experiments, both the asialo-PTX3$_r$ and the endo F3-PTX3$_r$ bound immobilized C1q 2−3 times more than the unmodified PTX3$_r$ (Figs 4A and B, middle panels). Protein concentration was normalized by Lowry. PTX3$_r$ samples were also subjected to ELISA titration, and concentration values were found identical to those obtained by Lowry, ruling out the fact that the observed increase in C1q binding might be ascribed to an increased affinity of the detection antibody for both asialo-PTX3$_r$ and endo-F3-PTX3$_r$ (data not shown).

PTX3 is a decameric protein stabilized by interprotomer disulfide bonds with a presumably high hydrodynamic volume and the potential to form supra-aggregates (*1*). Consistent with these features, PTX3$_r$ was eluted in size exclusion chromatography (SEC) as a protein with an estimated molecular weight of 900 kDa (Figs 4A and 4B, right panels). To assess whether α-(2→3,6,8,9)-neuramini-

dase or endoglycosidase F3 treatments might alter $PTX3_r$ oligomeric organization, we analyzed the elution profile of the protein in SEC. Both asialo-$PTX3_r$ and endo F3-$PTX3_r$ were eluted as a single peak with same retention time and apparent molecular weight (900 kDa) as those of the native protein, indicating that no major modification in $PTX3_r$ quaternary structure occurred after NeuNAc removal or deglycosylation (Figs 4A and B, right panels).

Asialo-$PTX3_r$ and endo F3-$PTX3_r$ binding to C1q was also analyzed in competition experiments. Microtiter plate wells were coated with $PTX3_r$, and the inhibition of C1q binding to the immobilized protein by asialo-$PTX3_r$ was measured. The results, expressed as both inhibition curves and IC50 values, showed that asialo-$PTX3_r$ inhibited the binding of C1q to immobilized $PTX3_r$ at one-third the concentration required for the untreated protein ($3.1 \pm 0.2$ $\mu$g/mL for asialo-$PTX3_r$ compared to $11.6 \pm 2.5$ $\mu$g/mL for $PTX3_r$, in Figure 5A), which is consistent with the direct binding experiments described above. Analogous results were achieved by measuring the inhibition of C1q binding to asialo-$PTX3_r$-coated wells ($2.9 \pm 0.4$ $\mu$g/mL for asialo-$PTX3_r$ compared to $8.9 \pm 0.5$ $\mu$g/mL for $PTX3_r$, in Figure 5B). Endo F3-$PTX3_r$ samples were assayed in the same experimental setting with comparable results (data not shown).

To further characterize the role of glycosylation on PTX3/C1q interaction, we investigated the binding to C1q of asialo-$PTX3_r$ and endo F3-$PTX3_r$ by means of real-time biomolecular interaction analysis with BIAcore. As shown in Figure 5C upper panel, when C1q was immobilized on the sensor chip, significant binding of $PTX3_r$ was observed. Kinetic analysis of the interaction between the two molecules allowed the calculation of a $K_{on}$ value of 1.98 ($\pm$ 0.03) $\times$ $10^4$ $M^{-1}$ $s^{-1}$ and a $K_{off}$ value of 9.39 ($\pm$ 0.09) $\times$ $10^{-4}$ $s^{-1}$ (considering a simple 1:1 interaction and PTX3 as a protomer). Under the same conditions, sensorgrams relative to asialo-$PTX3_r$ and endo F3-$PTX3_r$ exhibited higher RU signals (Figure 5C, middle and bottom panels, respectively); the corresponding calculated kinetic constants are $K_{on} = 2.05$ ($\pm$ 0.03) $\times$ $10^4$ $M^{-1}s^{-1}$ and $K_{off} = 7.62$ ($\pm$ 0.10) $\times$ $10^{-4}$ $s^{-1}$ for asialo-$PTX3_r$ and $K_{on} = 1.94$ ($\pm$ 0.02) $\times$ $10^4$ $M^{-1}s^{-1}$ and $K_{off} = 5.80$ ($\pm$ 0.15) $\times$ $10^{-4}$ $s^{-1}$ for endo F3-$PTX3_r$. Although differences among the measured parameters were relatively small, they were reproduced in a set of four independent experiments. Despite the $K_{on}$ invariancy among analyzed samples, we consistently observed a decrease of $K_{off}$ values as terminal NeuNAc residues or overall glycosidic moiety were removed from the protein. This behavior was in agreement with the binding experiments carried out at equilibrium, further indicating that deglycosylation stabilizes the PTX3/C1q complex, reducing its dissociation rate rather than accelerating molecules association.

*$PTX3_r$ Sialic Acid Content Affects Complement Activation.* We observed that both desialylation and deglycosylation equally enhanced $PTX3_r$ binding to C1q. As sialic acid has been described to play a key role in modulating glycoproteins activities (*39*), we analyzed the effect of desialylation on PTX3 complement activation.

$PTX3_r$ and asialo-$PTX3_r$ were immobilized on microtiter plates, and following incubation with normal human serum (NHS), activation of C4 and C3 was measured by ELISA. As shown in Figure 6A and B, the removal of sialic acid consistently induced an increase in both C4 and C3 deposition on asialo-$PTX3_r$ compared to that on $PTX3_r$ with increased C1q binding, as previously described. As a positive control of classical complement pathway (CCP) activation, immobilized IgMs were used. Analogous results were obtained with F3-PTX3 (data not shown).

With the aim of verifying whether sialylation status could affect the pathway through which PTX3 activates the complement system, C3 deposition on $PTX3_r$ and asialo-$PTX3_r$ was measured in the presence of the CCP inhibitors Mg-EDTA and EDTA or the C1q-inhibitory mAb85. Only the alternative complement pathway, that is neither the CCP nor the lectin pathways, can proceed in the absence of $Ca^{2+}$. No activation of C3 could be observed when Mg-EDTA or EDTA was added to the complement source, neither on $PTX3_r$ and asialo-$PTX3_r$ nor on IgM (Figure 6C). Furthermore, C3 deposition was totally abolished when the activation assay was performed in the presence of mAb85 (Figure 6C), thus indicating that sialic acid removal from PTX3 cannot shift the pentraxin-dependent complement activation toward pathways other than the classical one. In C1q-dependent haemolytic assays, fluid-phase PTX3 competes with C1q interaction to antibody-sensitized erythrocytes, thus inhibiting the complement classical pathway as revealed by a reduction of complement haemolytic activity (*8*). Asialo-$PTX3_r$ inhibited complement haemolytic activity at about half the concentration required for the unmodified protein (Figure 6D), indicating that the enhancement in C1q binding and complemnt activation observed upon the removal of sialic acid residues is maintained when the protein is in fluid-phase.

In an effort to assess the functional relevance of the enhanced complement activation by the deglycosylated PTX3, an air pouch model was used (*40*) where leukocytes recruitment is dependent on complement activation (Garlanda, unpublished data). In one experiment, the average number of recruited leukocytes in PTX3 mice was $51 \pm 6$ ($n = 3$), whereas the average number of recruited leukocytes in F3-PTX3 treated mice was $247 \pm 62$ ($n = 4$) ($p < 0.01$).

*Oligosaccharides Structure of PTX3 from Different Cellular Sources.* We extended our investigation into the PTX3 oligosaccharide structure to the naturally occurring protein. Endoglycosidases and exoglycosidases proved effective at assessing the $PTX3_r$ sugar type, as confirmed by mass spectrometry analysis. Thus, we exploited the analytical capacity of these enzymes to partially resolve the glycosylation of PTX3 purified from dendritic and 8387 cells stimulated with LPS and TNF$\alpha$, respectively. The natural protein from both cell types was resistant to endoglycosidase F1, whereas endoglycosidases F2 and F3 proved effective in reducing PTX3's apparent molecular weight (Figure 7A). These data showed that the natural protein is conjugated to complex-type sugars, analogous to $PTX3_r$. Interestingly, the susceptibility of natural PTX3 to endoglycosidase digestion appeared to be variable. In particular, a higher amount of $PTX3_{DC}$ retained glycosylation after endoglycosidase F2 hydrolysis with respect to $PTX3_{8387}$ or $PTX3_r$, suggesting that biantennary structures are a minor fraction of $PTX3_{DC}$ oligosaccharides. Moreover, the persistence of a large quantity of glycosylated $PTX3_{DC}$ after endoglycosidase F3 treatment indicates the presence of a higher proportion of tetrantennary structures (Figure 7A).

The susceptibility of PTX3 from either 8387 or dendritic cells to sequential monosaccharide hydrolysis by substrate-

specific exoglycosidases (Figure 7B) confirmed that the naturally occurring protein carries complex-type sugars, as does the recombinant one, and revealed the NeuNAc residues at the nonreducing terminal end of their antennae.

To evaluate the contribution of NeuNAc residues to C1q interaction, $PTX3_{8387}$ and $PTX3_{DC}$ samples were desialylated under nondenaturing conditions. Asialo-$PTX3_{8387}$ and asialo-$PTX3_{DC}$ were then assayed for their binding to C1q. Both desialylated $PTX3_{8387}$ and $PTX3_{DC}$ showed at least a 2-fold increase in C1q binding activity compared to that of the respective unmodified proteins (Figure 7C and D). These results match those obtained with $PTX3_r$ and allow us to conclude that sialic acid content affects PTX3/C1q interaction. It is noteworthy that unmodified PTX3 from the three different sources showed variable C1q binding (data not shown). Such a difference may be ascribed to the variations observed in the glycosylation status of the examined proteins (Figure 7A). Although we cannot rule out other possibilities, those shall be addressed in subsequent investigations.

*Conformational Analysis of PTX3 Oligosaccharides*. We evaluated the probability of contacts between biantennary oligosaccharides and the surface of the PTX3 *C*-terminus domain. A core-monofucosylated and disialylated biantennary oligosaccharide (Figure 8A), as the most abundant $PTX3_r$ glycan structure described above, was chosen for the analysis. The oligossaccharide chain was linked to Asn220 on a 3D model of the PTX3 *C*-terminus domain elaborated by homology modeling on the crystallographic structure of CRP (*35*). The sugar was then subjected to conformational analysis using dihedral angle driving and MC/SD procedures to guarantee an effective local sampling. Thirty three of the 400 oligosaccharide conformations collected showed the oligosaccharide chain contacting protein surface principally by the α-(1→6) antenna. In 96% of these solutions, sialic acid established hydrogen bonds with polar amino acids, and in the remaining 4%, it was involved in salt bridges with basic amino acids. Cluster analysis of the sialylated oligosaccharide conformations returned the three representative solutions shown in Figure 8B, where sialic acid interacts to Lys214, Glu252, Lys255, and Arg332. The removal of sialic acid from the terminal end of the disialylated biantennary oligosaccharide reduced the conformations interacting with exposed amino acids on protein surface to 14%. Monosaccharides of the mannosyl-chitobiose core are mainly involved in these contacts, whereas the antennae extend away from the protein surface. Representative solutions of the desialylated oligosaccharide are shown in Figure 8C. The proposed models in figures 8B and C suggest that sialic acid might exert a key role in modulating the anchoring of the PTX3 glycosidic moiety to the protein surface.

## DISCUSSION

We showed that oligosaccharides conjugated to the recombinant PTX3 were complex-type sugars, mainly consisting of biantennary fucosylated and variably sialylated structures. Our mass spectrometry data indicated that the unique glycosylation site at Asn220 is fully occupied in the native protein and ruled out the occurrence of O-linked oligosaccharides, confirming what was suggested in previous articles (*1*).

Recombinant PTX3 as well as PTX3 from fibrosarcoma cell line 8387 and from DC was similarly sensitive to exo and endoglycosidases digestion, thus indicating that the naturally occurring PTX3 also exhibits N-linked sialylated complex-type sugars. We observed intrinsic heterogeneity in the relative amount of bi, tri, and tetrantennary structures among the different species of PTX3 as indicated by the peculiar susceptibility of each species to endoglycosidase hydrolysis (Figure 7A). This result suggests that changes in the PTX3 glycosylation pattern might be ascribed to cell type and inflammatory stimulus.

The site of sugar attachment to PTX3 is located on Asn220 within the pentraxin domain that is known to mediate C1q recognition (*8*). We showed that enzymatically deglycosylated or desialylated PTX3 bound C1q 2−3-fold more than the unmodified protein, and we confirmed the specificity of this effect by competition experiments. The observed C1q binding enhancement did not appear to be determined by major rearrangements in the protein oligomeric status as potentially induced by sugars hydrolysis. SEC profiles of both deglycosylated and desialylated PTX3 matched that of the unmodified protein, indeed, retaining the apparent molecular weight of 900 kDa. However, we cannot rule out the possibility that changes in glycan composition may induce subtle modifications in PTX3 quaternary structure not detectable by SEC analysis.

We built a 3D model of the glycosylated PTX3 *C*-terminus, highlighting that oligosaccharides locally contact the PTX3 surface. Noteworthy sialic acid residues interact with polar and basic amino acids (Lys214, Glu252, Lys255, Arg332) at sites far from Asn220, carrying N-glycosylation. The removal of sialic acid from the nonreducing end of biantennary oligosaccharides induced glycan conformational changes that released their antennae away from the protein surface. We reported that either deglycosylation or desialylation equally enhanced PTX3 binding to C1q, indicating sialic acid as the main determinant of this effect. Our model proposes that the removal of sialic acid might determine new orientations of PTX3 oligosaccharides and analogous to deglycosylation, expose amino acids potentially relevant either to C1q recognition or to rearrangements of protein tertiary and quaternary structure.

The C1q binding enhancement observed for the recombinant protein upon removal of sialic acid was reproduced with the naturally occurring species ($PTX3_{8387}$ and $PTX3_{DC}$), thus indicating that desialylation also determines similar effects on the endogenous protein.

Because sialic acid plays a key role in modulating glycoprotein activity (*39*), we analyzed the effect of desialylation on PTX3 complement activation. It is known that PTX3 can both activate and inhibit the complement classical pathway depending on the way the protein is presented. Immobilized PTX3 induces complement activation as assessed by C3 and C4 deposition experiments, whereas the interaction of PTX3 with C1q in fluid phase inhibits complement cascade as established by the reduction of complement haemolytic activity (*8*). We observed a 2-fold increase in C3 and C4 deposition with desialylated PTX3 compared to that of the unmodified protein. This enhancement in complement activation indeed depends on PTX3/C1q interaction because it was blocked by inhibitories of the classical pathway. The effect of desialylation on PTX3 complement activation was also assessed in a C1q-dependent haemolytic assay. Consistently with the C1q binding experi-

ments, desialylated PTX3 inhibited complement cascade at about half the concentration required for the unmodified protein. These results suggest that the strengthened interaction with C1q observed upon removal of sialic acid is independent of the way the protein is presented, either immobilized or in fluid-phase. Furthermore, desialylation of PTX3 enhances both the activatory and inhibitory function of the protein on complement cascade.

Some explanations of the mechanism through which PTX3 glycosylation affects C1q binding were provided by kinetic analyses performed with the BIAcore system. Stoichiometry of the PTX3/C1q complex has not been defined yet, likely due to the complexity of interaction (*8*). BIAcore raw data were thus analyzed under the simple hypotheses of 1:1 interaction and PTX3 as a protomer. The observed differences among PTX3 glycosylation variants indicated that C1q binding strengthening produced by sugar removal was due to a decrease in the $K_{off}$ values. This result allowed us to conclude that deglycosylation stabilizes the PTX3/C1q complex, reducing the rate of its dissociation rather than increasing molecular association.

Complement activation is an enzymatic process that might be associated with amplification of interactions occurring early in the cascade. An example of this is provided by the mutagenesis study performed on CRP where a 2−3-fold enhancement in C1q binding, exhibited by some of the mutants, led to a 10 fold amplification in C3 deposition experiments (*41*). We observed a 2−3-fold enhancement in complement activation that reflects the stabilization of the asialo-PTX3/C1q complex and suggests that the nature of the interaction between asialo-PTX3 and C1q does not affect the serine protease activity of C1s and C1r. However, the increase described in complement activation is susceptible to induce more pronounced effects downstream in the inflammatory cascade. Consistent with this view, F3-PTX3 induces about a 5-fold enhancement of leucocytes recruitment than the unmodified protein in the air−pouch model (*40*), thus further indicating that the stabilization of the interaction of deglycosylated PTX3 with C1q is functionally relevant.

Protein-conjugated oligosaccharides can be processed in the extracellular environment by specific exoglycosidases; among these, neuraminidases appear to be particularly relevant because of their biological roles (*42*). Infact, several studies showed that different pathogens express neuraminidases on their surface during infection (*43*, *44*) and that natural immunity cells, such as polymorphonuclear leucocytes, also mobilize intracellular neuraminidases to the plasma membrane upon inflammatory stimuli (*45*). Here, we provide evidences that the PTX3 glycosylation status affects the interaction with C1q, and in this way, it is capable of modulating the activation of complement classic pathway. PTX3 has been functionally defined as a soluble pattern recognition receptor (SPRR) because it binds selected pathogens. The interaction of PTX3 with pathogens has the potential to promote complement opsonization, mediating microbicidal activity (*6*). Our study indicates that glycosylation might represent a strategy to tune PTX3 activity and paves the way for a new series of investigations aimed at establishing the biological relevance of PTX3 glycosylation in vivo.

## ACKNOWLEDGMENT

We thank Barbara Bottazzi and Ottaviano Serlupi Crescenzi for valuable discussions and advice.

## REFERENCES

1. Bottazzi, B., Vouret-Craviari, V., Bastone, A., De Gioia, L., Matteucci, C., Peri, G., Spreafico, F., Pausa, M., D'Ettorre, C., Gianazza, E., Tagliabue, A., Salmona, M., Tedesco, F., Introna, M., and Mantovani, A. (1997) Multimer formation and ligand recognition by the long pentraxin PTX3. Similarities and differences with the short pentraxins C-reactive protein and serum amyloid P component, *J. Biol. Chem. 272*, 32817−32823.
2. Breviario, F., D'Aniello, E., Golay, J., Peri, G., Bottazzi, B., Bairoch, A., Saccone, S., Marzella, R., Predazzi, V., Rocchi, M., Della Valle, G., Dejana, E., Mantovani, A., and Introna, M. (1992) Interleukin-1-inducible genes in endothelial cells. Cloning of a new gene related to C-reactive protein and serum amyloid P component, *J. Biol. Chem. 267*, 22190−22197.
3. Lee, G. W., Lee, T. H., and Vilcek, J. (1993) TSG-14, a tumor necrosis factor- and IL-1-inducible protein, is a novel member of the pentaxin family of acute phase proteins, *J. Immunol. 150*, 1804−1812.
4. Vouret-Craviari, V., Matteucci, C., Peri, G., Poli, G., Introna, M., and Mantovani, A. (1997) Expression of a long pentraxin, PTX3, by monocytes exposed to the mycobacterial cell wall component lipoarabinomannano, *Infect. Immun. 65*, 1345−1350.
5. Goodman, A. R., Cardozo, T., Abagyan, R., Altmeyer, A., Wisniewski, H. G., and Vilcek, J. (1996) Long pentraxins: an emerging group of proteins with diverse functions, *Cytokine Growth Factor Rev. 7*, 191−202.
6. Garlanda, C., Hirsch, E., Bozza, S., Salustri, A., De Acetis, M., Nota, R., Maccagno, A., Riva, F., Bottazzi, B., Peri, G., Doni, A., Vago, L., Botto, M., De Santis, R., Carminati, P., Siracusa, G., Altruda, F., Vecchi, A., Romani, L., and Mantovani, A. (2002) Nonredundant role of the long pentraxin PTX3 in anti-fungal innate immune response, *Nature 420*, 182−186.
7. Rovere, P., Peri, G., Fazzini, F., Bottazzi, B., Doni, A., Bondanza, A., Zimmermann, V. S., Garlanda, C., Fascio, U., Sabbadini, M. G., Rugarli, C., Mantovani, A., and Manfredi, A. A. (2000) The long pentraxin PTX3 binds to apoptotic cells and regulates their clearance by antigen-presenting dendritic cells, *Blood 96*, 4300−4306.
8. Nauta, A. J., Bottazzi, B., Mantovani, A., Salvatori, G., Kishore, U., Schwaeble, W. J., Gingras, A. R., Tzima, S., Vivanco, F., Egido, J., Tijsma, O., Hack, E. C., Daha, M. R., and Roos, A. (2003) Biochemical and functional characterization of the interaction between pentraxin 3 and C1q, *Eur. J. Immunol. 33*, 465−473.
9. Salustri, A., Garlanda, C., Hirsch, E., De Acetis, M., Maccagno, A., Bottazzi, B., Doni, A., Bastone, A., Mantovani, G., Beck Peccoz, P., Salvatori, G., Mahoney, D. J., Day, A. J., Siracusa, G., Romani, L., and Mantovani, A. (2004) PTX3 plays a key role in the organization of the cumulus oophorus extracellular matrix and in vivo fertilization, *Development 131*, 1577−1586.
10. Rusnati, M., Camozzi, M., Moroni, E., Bottazzi, B., Peri, G., Indraccolo, S., Amadori, A., Mantovani, A., and Presta, M. (2004) Selective recognition of fibroblast growth factor-2 by the long pentraxin PTX3 inhibits angiogenesis, *Blood 104*, 92−99.
11. Helenius, A., and Aebi, M. (2004) Roles of N-linked glycans in the endoplasmic reticulum, *Annu. Rev. Biochem. 73*, 1019−1049.
12. Dwek, R. A., Lellousch, A. C., and Wormald, M. R. (1995) Glycobiology: 'the function of sugar in the IgG molecule', *J. Anat. 187*, 279−292.
13. Rudd, P. M., Elliott, T., Cresswell, P., Wilson, I. A., and Dwek, R. A. (2001) Glycosylation and the immune system, *Science 291*, 2370−2376.
14. Spiro, R. G. (2002) Protein glycosylation: nature, distribution, enzymatic formation, and disease implications of glycopeptide bonds, *Glycobiology 12*, 43R−56R.
15. Martin, L. T., Marth, J. D., Varki, A., and Varki, N. M. (2002) Genetically altered mice with different sialyltransferase deficiencies show tissue-specific alterations in sialylation and sialic acid 9-O-acetylation, *J. Biol. Chem. 277*, 32930−32938.
16. Heegaard, P. M. (1992) Changes in serum glycoprotein glycosylation during experimental inflammation in mice are general, unrelated to protein type, and opposite changes in man and rat:

studies on mouse serum alpha 1-acid glycoprotein, alpha 1-esterase, and alpha 1-protease inhibitor, *Inflammation 16*, 631−644.
17. Mackiewicz, A., Dewey, M. J., Berger, F. G., and Baumann, H. (1991) Acute phase mediated change in glycosylation of rat alpha 1-acid glycoprotein in transgenic mice, *Glycobiology 1*, 265−269.
18. Chui, D., Sellakumar, G., Green, R., Sutton-Smith, M., McQuistan, T., Marek, K., Morris, H., Dell, A., and Marth, J. (2001) Genetic remodelling of protein glycosylation in vivo induces autoimmune disease, *Proc. Natl. Acad. Sci. U.S.A. 98*, 1142−1147.
19. Parekh, R. B., Dwek, R. A., Sutton, B. J., Fernandes, D. L., Leung, A., Stanworth, D., Rademacher, T. W., Mizuochi, T., Taniguchi, T., Matsuta, K., Takeuchi, F., Nagano, Y., Miyamoto, T., and Kobata, A. (1985) Association of rheumatoid arthritis and primary osteoarthritis with changes in the glycosylation pattern of total serum IgG, *Nature 316*, 452−457.
20. Tennent, G. A., and Pepys, M. B. (1994) Glycobiology of the pentraxins, *Biochem. Soc. Trans. 22*, 74−79.
21. Pepys, M. B., Rademacher, T. W., Amatayakul-Chantler, S., Williams, P., Noble, G. E., Hutchinson, W. L., Hawkins, P. N., Nelson, S. R., Gallimore, J. R., Herbert, J., Hutton, T., and Dwek, R. A. (1994) Human serum amyloid P component is an invariant constituent of amyloid deposits and has a uniquely homogeneous glycostructure, *Proc. Natl. Acad. Sci. U.S.A. 91*, 5602−5606.
22. Kiernan, U. A., Nedelkov, D., Tubbs, K. A., Niederkofler, E. E., and Nelson, R. W. (2004) Proteomic characterization of novel serum amyloid P component variants from human plasma and urine, *Proteomics 4*, 1825−1829.
23. Siebert, H. C., Andre, S., Reuter, G., Kaptein, R., Vliegenthart, J. F., and Gabius, H. J. (1997) Comparison between intact and desialylated human serum amyloid P component by laser photo CIDNP (chemically induced dynamic nuclear polarization) technique: an indication for a conformational impact of sialic acid, *Glycoconjugate J. 14*, 945−949.
24. Ashton, A. W., Boehm, M. K., Gallimore, J. R., Pepys, M. B., and Perkins, S. J. (1997) Pentameric and decameric structures in solution of serum amyloid P component by X-ray and neutron scattering and molecular modelling analyses, *J. Mol. Biol. 272*, 408−422.
25. Kottgen, E., Hell, B., Kage, A., and Tauber, R. (1992) Lectin specificity and binding characteristics of human C-reactive protein, *J. Immunol. 149*, 445−453.
26. Das, T., Sen, A., Kempf, T., Pramanik, S. R., Mandal, C., and Mandal C. (2003) Induction of glycosylation in human C-reactive protein under different pathological conditions, *Biochem. J. 373*, 345−355.
27. Das, T., Mandal, C., and Mandal, C. (2004) Variations in binding characteristics of glycosylated human C-reactive proteins in different pathological conditions, *Glycoconjugate J. 20*, 537−543.
28. Alles, V. V., Bottazzi, B., Peri, G., Golay, J., Introna, M., and Mantovani, A. (1994) Inducible expression of PTX3, a new member of the pentraxin family, in human mononuclear phagocytes, *Blood 84*, 3483−3493.
29. Laemmli, U. K. (1970) Cleavage of structural proteins during the assembly of the head of bacteriophage T4, *Nature 227*, 680−685.
30. Wray, W., Boulikas, T., Wray, V. P., and Hancock, R. (1981) Silver staining of proteins in polyacrylamide gels, *Anal. Biochem. 118*, 197−203.
31. Lowry, O. H., Rosenbrough, N. J., Farr, A. R., and Randall, R. J., (1951) Protein measurement with the Folin phenol reagent, *J. Biol. Chem. 193*, 265−275.
32. Amoresano, A., Siciliano, R., Orru, S., Napoleoni, R., Altarocca, V., De Luca, E., Sirna, A., and Pucci, P. (1996) Structural characterisation of human recombinant glycohormones follitropin, lutropin and choriogonadotropin expressed in Chinese hamster ovary cells, *Eur. J. Biochem. 242*, 608−618.
33. Dell, A., Khoo, K. H., Panico, M., McDowell, R. A., Etienne, A. T., Reason, A. J., and Morris, H. R. (1993) Mass spectrometry of carbohydrate-containing biopolymers, in *Glycobiology: A Practical Approach* (Fukuda, M., and Kobata, A., Eds.) pp 187−222, Oxford University Press, New York.
34. Roos, A., Nauta, A. J., Broers, D., Faber-Krol, M., Trouw, L. A., Drijfhout, W., and Daha, M. R. (2001) Specific inhibition of the classical complement pathway by C1q-binding peptides, *J. Immunol. 167*, 7052−7059.
35. Thompson, D., Pepys, M. B., and Wood, S. P. (1999) The physiological structure of human C-reactive protein and its complex with phosphocholine, *Structure 7*, 169−177.
36. Tarentino, A. L., and Plummer, T. H., Jr. (1994) Enzymatic deglycosylation of asparagine-linked glycans: purification, properties, and specificity of oligosaccharide-cleaving enzymes from *Flavobacterium meningosepticum*, *Methods Enzymol. 230*, 44−57.
37. Hashimoto, C., Cohen, R. E., Zhang, W. J., and Ballou, C. (1981) Carbohydrate chains on yeast carboxypeptidase Y are phosphorylated, *Proc. Natl. Acad. Sci. U.S.A. 78*, 2244−2248.
38. Harvey D. J., Martin R. L., Jackson K. A., Sutton C. W. (2004) Fragmentation of N-linked glycans with a matrix-assisted laser desorption/ionization ion trap time-of-flight mass spectrometer, *Rapid Commun. Mass Spectrom. 18*, 2997−3007.
39. Kelm, S., and Schauer, R. (1997) Sialic acids in molecular and cellular interactions, *Int. Rev. Cytol. 175*, 137−240.
40. Jeannin, P., Bottazzi, B., Sironi, M., Doni, A., Rursnati, M., Presta, M., Maina V., Magistrelli, G., Haeuw, J. F., Hoeffel, G., Thieblemont, N., Corvaia, N., Garlanda, C., Delneste, Y., and Mnatovani, A.., (2005) Complexity and complementarity of outer membrane protein A recognition by cellular and humoral innate immunity receptors, *Immunity 22*, 551−560.
41. Agrawal, A., and Volanakis, J. E. (1994) Probing the C1q-binding site on human C-reactive protein by site-directed mutagenesis, *J. Immunol. 152*, 5404−5410.
42. Roggentin, P., Schauer, R., Hoyer, L. L., and Vimr, E. R. (1993) The sialidase superfamily and its spread by horizontal gene transfer, *Mol. Microbiol. 9*, 915−921.
43. Takahashi, T., Suzuki, T., Hidari, K. I., Miyamoto, D., and Suzuki, Y. (2003) A molecular mechanism for the low-pH stability of sialidase activity of influenza A virus N2 neuraminidases, *FEBS Lett. 543*, 71−75.
44. Todeschini, A. R., Girard, M. F., Wieruszeski, J. M., Nunes, M. P., DosReis, G. A., Mendonca-Previato, L., and Previato, J. O. (2002) trans-Sialidase from *Trypanosoma cruzi* binds host T-lymphocytes in a lectin manner, *J. Biol. Chem. 277*, 45962−45968.
45. Cross, A. S., Sakarya, S., Rifat, S., Held, T. K., Drysdale, B. E., Grange, P. A., Cassels, F. J., Wang, L. X., Stamatos, N., Farese, A., Casey, D., Powell, J., Bhattacharjee, A. K., Kleinberg, M., and Goldblum, S. E. (2003) Recruitment of murine neutrophils in vivo through endogenous sialidase activity, *J. Biol. Chem. 278*, 4112−4120.

BI0607453